
Adapter-Augmented Bandits for Online Multi-Constrained Multi-Modal Inference Scheduling

Xianzhi Zhang^{1,2} Yue Xu¹ Yinlin Zhu¹ Di Wu¹ Yipeng Zhou² Miao Hu¹ Guocong Quan¹

Abstract

Multi-modal large language model (MLLM) inference scheduling enables strong response quality under practical and heterogeneous budgets, beyond what a homogeneous single-backend setting can offer. Yet online MLLM task scheduling is nontrivial, as requests vary sharply in modality composition and latent reasoning difficulty, while execution backends incur distinct, time-varying costs due to system jitter and network variation. These coupled uncertainties pose two core challenges: deriving semantically faithful yet scheduling-relevant multi-modal task representations, and making low-overhead online decisions over irreversible multi-dimensional budgets. Accordingly, we propose M^2 -CMAB (Multi-modal Multi-constraint Contextual Multi-Armed Bandit), a multi-adapter-enhanced MLLM inference scheduling framework with three components: (i) a CLS-attentive, frozen-backbone *Predictor* that extracts compact task representations and updates only lightweight adapters for action-specific estimation; (ii) a primal-dual *Constrainer* that maintains online Lagrange multipliers to enforce long-horizon constraints via per-round objectives; and (iii) a two-phase *Scheduler* that balances exploration and exploitation under irreversible budgets. We establish a regret guarantee under multi-dimensional knapsack constraints. On a composite multimodal benchmark with heterogeneous backends, M^2 -CMAB consistently outperforms state-of-the-art baselines across budget regimes, achieving up to 14.18% higher reward and closely tracking an oracle-aided upper bound. Codes are available at <https://anonymous.4open.science/r/M2CMAB/>.

1. Introduction

Multi-modal large language models (MLLMs) have achieved remarkable success in jointly reasoning over text, images, audio, and variable-modal inputs (Xu et al., 2025; Liu et al., 2025). Advanced MLLM families, such as the Qwen-VL (Bai et al., 2025a;b) and LLaVA series (Li et al., 2024a;b) with multiple variants, can ingest heterogeneous sensory inputs and generate richly grounded responses, fueling increasingly diverse modality compositions and service-level requirements (Fei et al., 2025; Li et al., 2025b). In practice, cloud-scale deployment benefits from abundant compute and larger models, often delivering stronger response quality and robustness, whereas on-device deployment favors lightweight models that are cheaper to run and better suited for low-latency and privacy-sensitive operation. The collaboration of them offers a pragmatic paradigm, enabling real-world inference streams to achieve strong quality under practical cost constraints.

Despite this promise, resource-constrained deployment makes MLLM inference scheduling a fundamental problem (Li et al., 2025a). Incoming requests vary in modality composition and reasoning difficulty, giving rise to diverse service-level requirements that span quality of responses and budget consumption (Xia et al., 2024; Li, 2025). Meanwhile, execution backends exhibit substantially different performance-cost profiles, characterized by distinct model capacity, pricing, throughput, or network-dependent latency (Yang et al., 2024). As illustrated in Fig. 1, these coupled heterogeneities are reflected in average reward (response quality), latency, and monetary cost across on-device MLLMs and cloud APIs under a mixed multi-modal task trace. We thus ask: *How can we dynamically schedule MLLM inference across heterogeneous backends to maximize expected inference reward under stringent budgets?* Realizing this goal entails several core challenges.

The first bottleneck lies in representing inference tasks in both semantically faithful and scheduling-relevant. On the task side, real-world requests differ in modality composition, input scale, and latent reasoning difficulty, which can be heavy-tailed even within a single domain (Yuan et al., 2025; Yang et al., 2025). On the execution side, the observed inference results are confounded by stochastic decoding and

¹School of Computer Science and Engineering, Sun Yat-sen University, Guangzhou, 510006, China. ²School of Computing, Macquarie University, NSW 2109, Australia. Correspondence to: Di Wu <wudi27@mail.sysu.edu.cn>.

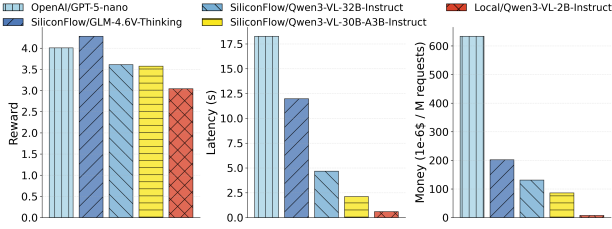


Figure 1. Comparison of reward, latency, and monetary cost across MLLM inference backends on a mixed multi-modal task trace.

system jitter, while end-to-end budget consumptions further entangle model compute with exogenous noise (e.g., network variation and time-varying on-device GPU contention), yielding non-stationary and drifting runtime patterns. Some handcrafted features (Fu et al., 2024; Yuan et al., 2025) or coarse statistics (e.g., token-count surrogates (Fu et al., 2024), modality indicators (Yuan et al., 2025; Yang et al., 2025), and static device profiles (Yang et al., 2024)), are brittle proxies of difficulty and cost, and can break under distribution or modality shifts (Chen et al., 2025; Oh et al., 2025). This motivates leveraging MLLMs themselves to produce task-level representations that summarize multi-modal semantics and implicit difficulty cues (Tu et al., 2025; Wu et al., 2025; Wang et al., 2025), enabling more reliable online scheduling under uncertainty.

A second obstacle arises from the online scheduling itself. First, online collaboration scheduling typically runs at the local and must stay on the critical path, leaving little headroom for expensive decision making (Ma et al., 2025). Methods that either depend on auxiliary MLLM-based embedding extraction (Oh et al., 2025; Tu et al., 2025; Wu et al., 2025), or require model tuning/adaptation before each decision (Huang et al., 2025; Ge et al., 2025), can incur non-trivial computation and inference overhead (Zhou et al., 2025). Second, decisions are inherently *irreversible* under strict budgets: resource slack is consumed on the fly, while future requests and their modality mix remain unknown. Consequently, heuristic or reinforcement-learning-style policies may over-explore and exhaust budgets early, yet offer limited guarantees on long-horizon constraint satisfaction (Pei et al., 2025; Yang et al., 2025). These challenges call for a principled online learning framework that enables lightweight per-round decisions while explicitly controlling cumulative resource consumption (Jia et al., 2025; Agrawal & Devanur, 2016; Han et al., 2023).

To tackle the above challenges, we formulate resource-constrained MLLM inference scheduling as a multi-modal, multi-constraint contextual bandit with knapsacks (M^2 -CBwK) problem. This formulation extends the classic CBwK framework (Han et al., 2023; Jia et al., 2025) by explicitly modeling structured multi-modal contexts and heterogeneous cost dimensions intrinsic to real MLLM deployments. Based on this abstraction, we develop M^2 -CMAB

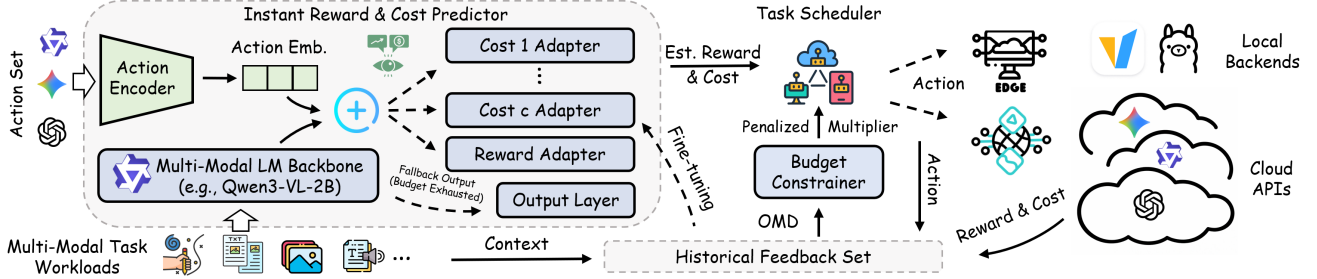
(Multi-modal Multi-constraint Contextual Multi-Armed Bandit), an online MLLM task scheduling framework consisting of three components: a multi-adapter-enhanced *Pre-dictor*, an online primal-dual-based *Constrainer*, and a two-phase *Scheduler* for exploration-exploitation. We highlight the main contributions as follows.

- ❶ **Efficient MLLM Representation.** We extract a compact CLS-attentive task context from a frozen MLLM and update only lightweight reward/cost adapters online, enabling low-overhead, action-specific prediction while preserving generative capability of the local backend.
- ❷ **Decoupled Long-Horizon Constraint Control.** We maintain online Lagrange multipliers via a primal-dual update, decoupling cumulative constraints enforcement from per-round decisions under irreversible, multi-dimensional budgets.
- ❸ **Efficient Contextual Scheduling.** We propose a contextual exploration-exploitation policy that jointly uses multi-modal context and constraint feedback, and establish a regret guarantee under multiple knapsack constraints.
- ❹ **Realistic Benchmark and Strong Empirical Results.** We build a benchmark with five backends, six datasets, and seven methods, and show M^2 -CMAB outperforms other state-of-the-art scheduling methods, achieving up to 14.18% higher average reward, and most closely matches an oracle-aided counterpart that uses perfect per-round observed information.

2. Preliminary and Problem Formulation

Our study focuses on designing an online scheduling algorithm to address dynamic decision-making problems for MLLM inference tasks. At each round $t \in \{1, \dots, T\}$, the scheduling algorithm receives an incoming task with the multi-modal context $\mathbf{x}^t = \{\mathbf{x}_\omega^t\}_{\omega \in \Omega}$, where Ω denotes the set of available modalities (e.g., text, vision, audio, and auxiliary metadata). For each modality ω , $\mathbf{x}_\omega^t \in \mathbb{R}^{d_\omega^{\text{in}} \times d_\omega^{\text{tok}}}$ represents its token-level embedding, where d_ω^{tok} denotes the number of tokens and d_ω^{in} denotes the per-token embedding dimensionality for modality ω , jointly forming the task-level multi-modal prompt input to the MLLM.

Given the context \mathbf{x}^t , the scheduler selects an action $a^t \in \mathcal{A}$ from the action space (e.g., a specific backend combining the execution environment, model choice, and reasoning mode) according to a learnable policy $\pi(\cdot | \mathbf{x}^t)$. The objective of the policy is to maximize the overall quality of service (QoS), quantified as the expected cumulative reward $\mathbb{E} \left[\sum_{t=1}^T r_{a^t}^t \right]$, while satisfying multiple long-term budget constraints $\Phi \in \mathbb{R}_+^C$ across C resource dimensions (e.g., monetary cost and latency). Accordingly, the problem is formulated as a multi-modal, multi-constraint contextual bandit with knapsacks (M^2 -CBwK) problem, denoted by $\mathbb{P}1$, where $\mathcal{R}(\cdot, \cdot)$ denotes the reward function induced by the selected action and the observed context, $\varphi_a^t = \mathcal{C}(a, \mathbf{x}^t)$ represents


 Figure 2. Overview of the M^2 -CMAB decision-making pipeline.

the corresponding resource consumption vector in round t , and $\mathbb{1}$ represents the all-ones vector. The constraints in (1b) are applied component-wise and are dimensionless. Finally, Ω denotes the set of supported modalities that together constitute the multi-modal context \mathbf{x}^t .

$$\mathbb{P}1 : \max_{\pi} \mathbb{E} \left[\sum_{t=1}^T r_a^t \right], \quad (1a)$$

$$\text{s.t.} \quad \sum_{t=1}^T \frac{\varphi_a^t}{\Phi} \leq \mathbb{1}, \quad (1b)$$

$$r_a^t := \mathcal{R}(a, \mathbf{x}^t), \quad \varphi_a^t := \mathcal{C}(a, \mathbf{x}^t), \quad (1c)$$

$$a \sim \pi(\cdot | \mathbf{x}^t), \quad (1d)$$

$$\mathbf{x}^t = \{\mathbf{x}_{\omega}^t\}_{\omega \in \Omega}, \quad \forall t. \quad (1e)$$

The online task offloading problem $\mathbb{P}1$ captures the intrinsic dynamics of sequential multi-modal inference tasks under uncertainty. In this setting, MLLM inference outcomes are inherently stochastic: for a given context \mathbf{x}^t and action a^t , the realized reward and cost depend on complex task-backend interactions and are only revealed after execution. Meanwhile, offloading decisions must be made irrevocably without access to future task arrivals, requiring the scheduler to adapt online while jointly managing multiple limited macro-budgets so that costly resources are reserved for sufficiently complex tasks. These characteristics give rise to two core challenges. **C1 (Uncertain payoff modeling)** arises from the difficulty of accurately characterizing $\mathcal{R}(a^t, \mathbf{x}^t)$ and $\mathcal{C}(a^t, \mathbf{x}^t)$, since reward and cost distributions induced by MLLM inference admit no closed-form expressions. **C2 (Non-myopic budget coupling)** stems from the fact that greedy per-round optimization may prematurely exhaust unrecoverable budgets, resulting in suboptimal long-term QoS performance. Additionally, we summarize the key notations in Table 1 in Appendix A.

3. M^2 -CMAB Design

Our M^2 -CMAB framework to solve $\mathbb{P}1$, illustrated in Fig. 2, consists of three coupled components. The *Predictor* uses an adapter-based MLLM to estimate the reward r^t and cost vector φ^t from the given action and context, addressing uncertain payoff modeling (C1). The *Constrainer* then applies

budget-aware penalties to regulate per-round resource usage, mitigating non-myopic budget coupling (C2). Finally, the *Scheduler* combines the predicted rewards and penalized costs to make the exploration-exploitation decision.

3.1. Reward and Cost Predictor Design

Accurate reward and cost prediction is central to efficient online decision-making in M^2 -CMAB, yet extracting task-aligned embeddings from MLLMs for scalar regression is non-trivial. A straightforward approach is to fine-tune the backbone MLLM model (Ge et al., 2025; Huang et al., 2025). While effective for certain downstream tasks, directly fine-tuning backbone models for reward and cost regression is often mismatched to online decision-making settings. First, trajectory-level feedback in online scheduling is typically noisy and non-stationary, making fine-tuned embeddings prone to overfitting transient patterns and degrading representation stability over time. Second, repeated fine-tuning incurs substantial computational and system overhead, rendering it impractical for scenarios that require fast adaptation training and frequent prediction.

Freezing the backbone alleviates these issues but introduces an additional challenge. In frozen-backbone settings, directly extracting embeddings from the final output token remains suboptimal, as its hidden state is primarily optimized for next-token prediction and does not reliably summarize global task semantics. This mismatch becomes more pronounced in long or multi-modal contexts, where scalar reward and cost regression depends critically on consistent task-level representations rather than generative diversity.

To address these challenges, we adopt a CLS-attentive multi-adapter-based prediction pipeline built on one frozen backbone. Specifically, we freeze the parameters ϑ of MLLM backbone $f_{\vartheta}(\cdot)$ to preserve its generative capability and representation consistency. To avoid directly using the final token output, an explicit [CLS] token is introduced as a global semantic anchor at the beginning of the multi-modal context input tokens \mathbf{x}^t . Its multi-head self-attention weights $\alpha_h^t = \mathbf{I}_h^t[\text{CLS}, :]$ are then used to perform attention-based pooling over the hidden states \mathbf{H}^t , where $\mathbf{H}^t \in \mathbb{R}^{L \times d_{\text{hid}}}$ and $\mathbf{I}^t \in \mathbb{R}^{H \times L \times L}$ are extracted from the last output layer of the frozen backbone, thereby yielding

a task hidden representation $z_x^t = f_\vartheta(\mathbf{x}^t)$ aligned with context semantics.

Given the task representation z_x^t , prediction is performed by conditioning on both the contextual information and the selected action. To this end, we concatenate z_x^t with the action embedding z_a , obtained from a language modality embedder, and feed the resulting representation into a set of lightweight adapters $\mathcal{F}_\theta(z_a || z_x^t)$, parameterized by θ_r^t and $\{\theta_\varphi^{t,(c)}\}_{c=1}^C$ for reward and per-dimension constraint estimation, respectively. These adapters serve as task-specific heads that map the shared representation to scalar reward and cost estimates, enabling efficient and stable prediction without modifying the frozen backbone parameters.

Specifically, the reward adapter can be formulated $\hat{r}_a^t = \hat{\mathcal{R}}(a, \mathbf{x}^t; \Theta_r^t)$, where $\Theta_r^t = \{\vartheta, \theta_r^t\}$ includes the frozen MLLM backbone parameters and the trainable adapter parameters for reward regression. Likewise, for C budget-constraint dimensions (e.g., monetary cost, latency, energy), we assign each dimension c an independent cost adapter $\hat{\varphi}_a^{t,(c)} = \hat{\mathcal{C}}(a, \mathbf{x}^t; \Theta_\varphi^{t,(c)})$, producing the cost vector $\hat{\varphi}_a^t$ that characterizes the estimated per-round resource consumption for action a with parameter $\Theta_\varphi^{t,(c)} = \{\vartheta, \theta_\varphi^{t,(c)}\}$.

To train these predictors, we adopt a unified regularized least-squares objective. Let \mathcal{F}_θ denote either the reward predictor or a cost predictor for dimension c , and let y^τ represent its corresponding supervision signal, i.e., reward r^τ or cost $\varphi^{\tau,(c)}$. The adapter parameters θ are updated by

$$\min_{\theta} \mathcal{J}(\theta) = \frac{1}{2|\Upsilon^t|} \sum_{\tau < t} (\mathcal{F}_\theta^\tau - y^\tau)^2 + \frac{\eta}{2} \|\theta - \theta^0\|_2^2, \quad (2)$$

where $\Upsilon^t = \{(r^\tau, \varphi^\tau, a^\tau, \mathbf{x}^\tau) \mid \tau < t, \tau \in \mathbb{N}_+\}$ is the historical set of observations before round t , θ^0 is the initialization of the adapter parameters, and $\eta > 0$ is the regularization coefficient. Instantiating (2) with $(\mathcal{F}_\theta, y^\tau)$ equal to (\hat{r}_a^τ, r^τ) gives the reward regression loss $\mathcal{J}_r(\theta_r^t)$, while choosing $(\hat{\varphi}_a^{\tau,(c)}, \varphi^{\tau,(c)})$ gives the cost loss $\mathcal{J}_\varphi^{(c)}(\theta_\varphi^{t,(c)})$ for each constraint c . Implementation details of the reward and cost predictors are deferred to Appendix B.

3.2. Long-Term Constrainer Design

To address challenge C2, we introduce a *Constrainer* that decouples time-dependent budget constraints via an online queue-based optimization framework (Ouyang et al., 2023; Zhang et al., 2025), enabling per-round budget allocation in $\mathbb{P}1$. Specifically, the long-term budget constraint in Eq. (1b) can be reformulated as a queue-recursion process by associating each constraint with a Lagrange multiplier $\lambda^t \in \mathbb{R}_+^C$ at round t . Under this formulation, the cumulative objective in Eq. (1a) admits a Lagrangian form $\mathcal{L}(a, \lambda) = \sum_{t=1}^T \mathcal{L}^t(a, \lambda^t)$, where the per-round La-

grangian function is given by

$$\mathcal{L}^t(a, \lambda^t) = -r_a^t + \left\langle \frac{\varphi_a^t}{\Phi} - \frac{1}{T}, \lambda^t \right\rangle. \quad (3)$$

Here, $\Phi \in \mathbb{R}_+^C$ denotes the total budget vector, $\varphi_a^t \in \mathbb{R}_+^C$ represents the per-round resource consumption, and $\langle \cdot, \cdot \rangle$ is the standard inner product. This reformulation converts $\mathbb{P}1$ into a saddle-point problem that maximizes reward while penalizing budget violations, $\min_a \max_\lambda \mathcal{L}(a, \lambda)$ s.t. (1c) – (1e). Importantly, the use of Lagrange multipliers enables temporal decoupling, allowing the optimization to be carried out on a per-round basis by focusing on $\mathcal{L}^t(a^t, \lambda^t)$.

To update the dual variables online, we apply the online mirror descent (OMD) algorithm (Hazan, 2016; Shalev-Shwartz, 2012), which performs iterative updates over the dual domain by minimizing the per-round objective:

$$\mathcal{D}^t(\lambda^t) = \max_a \left(r_a^t - \left\langle \frac{\varphi_a^t}{\Phi} - \frac{1}{T}, \lambda^t \right\rangle \right). \quad (4)$$

The dual variable λ^t is constrained to the convex set $\mathcal{V} = \{\lambda \in \mathbb{R}_+^C : \|\lambda\|_1 \leq \Lambda\}$, where $\Lambda > 0$ specifies the radius of the feasible region. With the feasible set \mathcal{V} determined, the *Constrainer* updates the dual variable λ^{t+1} at each subsequent round according to

$$\lambda^{t+1} = \arg \min_{\lambda \in \mathcal{V}} \left(\left\langle \nabla \mathcal{D}^t(\lambda^t), \lambda \right\rangle + \frac{\mathcal{B}(\lambda, \lambda^t)}{\varrho_t} \right), \quad (5)$$

where $\mathcal{B}(\cdot, \cdot)$ denotes the Bregman divergence induced by the negative-entropy generating function (Han et al., 2023), and ϱ_t is the step size of the OMD. This update corresponds to a mirror-descent step that balances the instantaneous dual gradient and proximity to the previous iterate.

Overall, the *Constrainer* incorporates long-term budget constraints into per-round reward maximization by dynamically adjusting the dual variables λ^t , thereby imposing adaptive and forward-looking penalties on budget consumption.

3.3. Task Scheduler Design

Leveraging prediction results and decoupled constraints, the final component of M^2 -CMAB assigns each action a scalar score, upon which a two-phase Contextual Multi-Armed Bandit (CMAB) framework is employed to balance the exploration-exploitation trade-off and make final online scheduling decisions under uncertainty.

3.3.1. INITIAL PHASE

The target of the initial phase is to establish the space $\mathcal{V} = \{\lambda \in \mathbb{R}_+^C : \|\lambda\|_1 \leq \Lambda\}$ for *Constrainer*, so that the budget consumption can be properly penalized in the exploration-exploitation phase. Inspired by Han et al. (2023), we employ a regression-based procedure to estimate λ . The initial phase

lasts $(A + 1) \cdot T_0$ rounds to evaluate Λ , where A denotes the size of the action space and T_0 is a hyper-parameter specifying the number of times each action is selected. To ensure that the OMD algorithm achieves $O(\sqrt{T})$ regret bounds, our preferred choice is to set $\Lambda = T \cdot \frac{\text{OPT}}{\Phi_{\min}}$ (Lemma D.6), where OPT is defined in Definition D.2 and $\Phi_{\min} = \|\Phi^{-1}\|_{\infty}$. However, OPT cannot be solved accurately in an online scenario. Therefore, we employ a regression algorithm in the initial phase including $(A + 1) \cdot T_0$ rounds to evaluate Λ . Generally speaking, there are two steps in the initial phase.

Stage ①: For the first $A \cdot T_0$ rounds, we play different A actions in CMAB evenly for T_0 times to gather historical records set $\Upsilon^{A \cdot T_0} = \{(r^\tau, \varphi^\tau, a^\tau, \mathbf{x}^\tau) \mid \tau \leq A \cdot T_0, \tau \in \mathbb{N}_+\}$. With the historical records, we can train an adapter as an oracle to predict the reward and cost $\hat{r}_a^t, \forall a \in \mathcal{A}, \forall t \in \mathcal{T}_0$, where $\mathcal{T}_0 = \{t : A \cdot T_0 + 1 \leq t \leq (A + 1) \cdot T_0\}$.

Stage ②: For the latter total T_0 rounds, *i.e.*, we select actions a^t randomly and observe the reward r^t , where $t \in \mathcal{T}_0$. Then, we use the observed history's prediction model to estimate $\hat{\text{OPT}}(T_0)$ by solving the linear programming problem (6), where \mathbf{o} is the solution matrix. Additionally, T denotes the maximum number of training rounds, C is the total number of constraints, $\mathbb{1}$ represents the all-ones vector, and Φ denotes the budget vector across all constraints. The term $\mathcal{M}(T_0)$ characterizes the aggregated estimation uncertainty arising from both the reward and cost regression oracles. Once all required parameters are obtained, the estimated value $\hat{\text{OPT}}(T_0)$ can be computed by solving the linear program in Eq. (6) using a standard linear programming solver.

$$\hat{\text{OPT}}(T_0) = \max_{\mathbf{o} \in \mathcal{O}} \frac{1}{T_0} \sum_{t \in \mathcal{T}_0} \sum_{a \in \mathcal{A}} o_a^t \hat{\mathcal{R}}(a, \mathbf{x}^t; \Theta_r^t), \quad (6a)$$

$$\text{s.t.} \quad \sum_{t \in \mathcal{T}_0} \sum_{a \in \mathcal{A}} o_a^t \frac{\hat{\mathcal{C}}(a, \mathbf{x}^t; \Theta_\varphi^t)}{T_0 \Phi} \preceq \frac{\mathbb{1}}{T} + 2 \frac{\mathcal{M}(T_0)}{\Phi}, \quad (6b)$$

$$\mathcal{M}(T_0) = \sqrt{A (\mathcal{E}_r(T_0) + d \mathcal{E}_c(T_0)) + 4 \frac{\log(TC)}{T_0}}. \quad (6c)$$

Upon obtaining the estimated value $\hat{\text{OPT}}(T_0)$, we set $\Lambda = \frac{T}{\Phi_{\min}} \left(\hat{\text{OPT}}(T_0) + \mathcal{M}(T_0) \right)$. Consequently, the estimated value of Λ effectively controls the deviation induced by estimation uncertainty. The detailed procedure for determining Λ is provided in Alg. 1 in Appendix C.

3.3.2. EXPLORATION-EXPLOITATION PHASE

In this phase, *Scheduler* leverages the outputs of *Predictor* and *Constrainer* to make online decisions. In general, the exploration-exploitation phase consists of three steps in each round $t \in ((A + 1) \cdot T_0, T]$, as follows:

Step ① (Generating Action Scores): After observing multi-

modal context \mathbf{x}^t , *Scheduler* receives \hat{r}_a^t and $\hat{\varphi}_a^t$ from *Predictor* and the current multiplier λ^t from *Constrainer* for all $a \in \mathcal{A}$, and then computes the predicted per-round Lagrangian as the action score:

$$\mathcal{S}^t(a) = \hat{r}_a^t - \left\langle \frac{\hat{\varphi}_a^t}{\Phi} - \frac{1}{T}, \lambda^t \right\rangle, \forall a \in \mathcal{A}. \quad (7)$$

Step ② (Selecting the Optimal Action): Based on the estimated action scores, *Scheduler* assigns exploration-exploitation sampling probabilities to all arms. Let a_{\max}^t denote the action with the highest score $\mathcal{S}^t(a_{\max}^t)$; the probability of sampling other action is then computed as:

$$\mathcal{P}^t(a) = \frac{1}{A + \rho (\mathcal{S}^t(a_{\max}^t) - \mathcal{S}^t(a))}, \forall a \in \mathcal{A} \setminus a_{\max}^t, \quad (8)$$

where ρ is a hyper-parameter controlling the extent to which M^2 -CMAB favors exploitation over exploration. When ρ is small, $\mathcal{P}^t(a)$ approaches $\frac{1}{A}$, indicating that M^2 -CMAB samples actions more uniformly and thus prefers exploration. The selection probability of a_{\max}^t is given by

$$\mathcal{P}^t(a_{\max}^t) = 1 - \sum_{a \in \mathcal{A}, a \neq a_{\max}^t} \mathcal{P}^t(a). \quad (9)$$

The final action $a^t \sim \mathcal{P}^t(\cdot)$ is sampled according to the probability distribution defined in Eqs. (8) and (9), under the context \mathbf{x}^t and the variable λ^t .

Step ③ (Updating Penalties): M^2 -CMAB leverages *Constrainer* to update the new dual variable vector λ^{t+1} based on Eq. (5), which will be used for budget allocation in the next round on the fly. This process navigates a dynamic stream of multi-modal inference tasks, where each task is strategically scheduled to maximize inference performance while adhering to resource constraints. The details of M^2 -CMAB are shown in Alg. 2 in Appendix D.

4. Regret Analysis

We next analyze the regret performance of M^2 -CMAB. Following (Zhang et al., 2025), we define OPT in Definition D.2 in Appendix D as the optimal expected per-round reward achievable under the prescribed resource budget constraints. Let $T \cdot \text{OPT}$ denote an upper bound on the cumulative optimal reward over T rounds in the online setting (Agrawal & Devanur, 2016). The regret of M^2 -CMAB is defined as $\text{Reg}(T) = T \cdot \text{OPT} - \mathbb{E} \left[\sum_{t=1}^T r_a^t \right]$, and we establish the following regret guarantee.

Theorem 4.1. *Let T denote the total number of scheduling rounds, T_0 the number of times each action is selected in the initial phase, and A the number of actions. Define*

$\Phi_{\min} = |\Phi^{-1}|_{\infty}$. Then, we have:

$$\text{Reg}(T) \lesssim \left(\frac{T \text{OPT}}{\Phi_{\min}} + 1 \right) \left(AT_0 + \sqrt{AT[\text{Reg}^r(T) + \text{Reg}^c(T) + \log(CT)]} \right), \quad (10)$$

where $\Phi_{\min} > \max\{(A+2)T_0, T\mathcal{M}(T_0)\}$ characterizes the feasible choice of T_0 and ensures that all budget constraints are satisfied. Here, $\mathcal{M}(\cdot)$ is defined in (6c). Moreover, $\text{Reg}^r(T)$ and $\text{Reg}^c(T)$ denote the cumulative regrets incurred by the reward and cost predictors, respectively, with respect to the optimal regression functions $\hat{\mathcal{R}}^*(a, \mathbf{x})$ and $\hat{\mathcal{C}}^*(a, \mathbf{x})$ over T rounds.

Proof. The detailed proof is provided in Appendix D. \square

Remark 4.2 (Discussions and Open Issues). The regret bound in Theorem 4.1 is modular with respect to the choice of the reward and cost estimators and holds for any estimator achieving sublinear estimation regret (Wu et al., 2015). Under this abstraction, existing results on GP-based predictors with kernelized confidence bounds imply that, assuming unbiased cost estimation, the induced estimation regret is on the order of $O(T^{3/4}(\log T)^{1/4})$ (Zhang et al., 2025). In a similar spirit, prior work on neural contextual bandits indicates that neural estimators can also achieve sublinear regret (e.g., $\tilde{O}(\sqrt{T})$) under appropriate regularity and over-parameterization assumptions when coupled with confidence-based exploration mechanisms (Li et al., 2025c). Extending such estimation regret guarantees to more general MLLM-based predictors under the decoupled scheduling scheme considered in this work remains an open problem.

5. Performance Evaluation

This section presents the experimental methodology for evaluating the proposed MLLM scheduling framework. Specifically, we aim to answer three questions: **Q1:** How robustly the framework performs under different budget regimes and task data distributions; **Q2:** How sensitive the framework is to key hyperparameters of *Scheduler*; **Q3:** How individual design adapters contribute to the final performance.

5.1. Benchmark

We build a trace-driven online multi-modal inference benchmark based on execution traces measured across multiple heterogeneous backends, comprising six datasets in total: five individual datasets and one composited-task dataset. Due to space constraints, some detailed descriptions of the benchmark setup are provided in Appendix E.

Backends. The benchmark consists of five different execution backends for each incoming task, covering both

local and cloud-based MLLMs. Specifically, the local execution options include lightweight models deployed on-device, while the cloud execution options comprise large-scale, reasoning-enhanced models provided by commercial platforms, spanning diverse choices in model scale, architecture (mixture-of-experts (MoE) vs. non-MoE), inference mode (thinking or not), and deployment platform.

Datasets. Our evaluation uses six datasets, including five representative individual datasets covering diverse tasks and modality requirements, as well as one composited-task dataset: InfoVQA (Mathew et al., 2021), GSM8K (Cobbe et al., 2021), SimpleVQA (Cheng et al., 2025), CoQA (Reddy et al., 2019), and AI2D (Kembhavi et al., 2016). These datasets span a diverse set of tasks, including multi-turn dialogue and reading comprehension (e.g., CoQA), mathematical reasoning (e.g., GSM8K), multi-modal question answering and diagram-based visual reasoning (e.g., SimpleVQA and AI2D), as well as knowledge-intensive visual understanding (e.g., InfoVQA). In addition to evaluating each dataset individually, we merge them to form a unified, large-scale dataset (COMPOSITE), enabling comprehensive evaluation across heterogeneous domain tasks. In evaluation, the measured inference traces of each dataset are split into two disjoint subsets. One half is used for offline adapter preparation, with an 80/20 split for training and validation, while the other half is reserved for online evaluation, where tasks are randomly permuted and then revealed sequentially for online decision making and parameter updates (Zhang et al., 2026).

Inference Metadata. Following the protocol of Yuan et al. (2025), we execute each task instance on candidate execution models and record the resulting inference metadata. System performance is evaluated along three dimensions: **1 Inference quality.** Response quality is quantified by a normalized reward $r \in [1, 5]$, where responses from different task types are mapped to a unified five-level quality scale to ensure consistency across datasets. **2 Latency.** Latency φ_{LATENCY} measures the end-to-end inference delay, including computation and network transmission when applicable. **3 Monetary cost.** Monetary cost φ_{COST} measures the economic expense of inference execution. For local execution, it reflects energy consumption translated into cost, whereas for cloud execution it includes token-based billing and modality-specific charges. Additional details of the inference metadata are provided in Appendix E.

Baselines. We evaluate our approach against several representative baselines: **1 Random**, which selects an execution backend uniformly at random in each round; **2 Latency-first**, which greedily selects the execution model with the lowest predicted latency according to our trained latency predictor; **3 Money-first**, which greedily selects the execution model with the lowest predicted monetary cost using

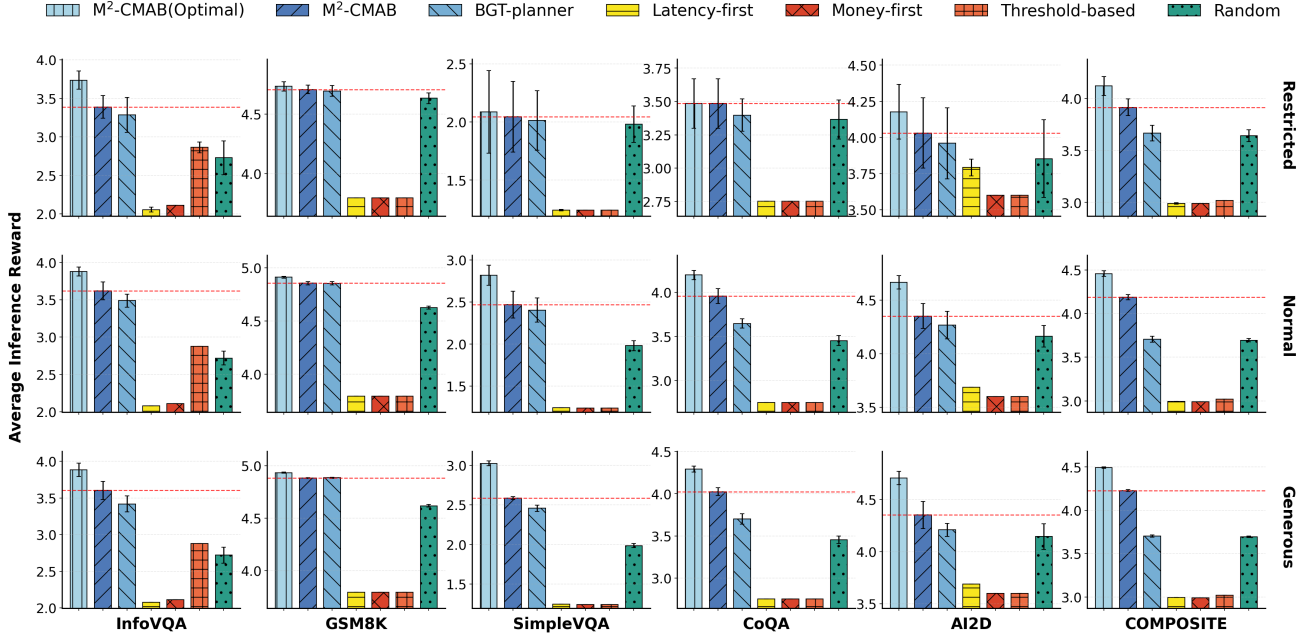


Figure 3. Average inference reward of M^2 -CMAB and baselines across six datasets and three budget regimes.

our trained cost predictor; ④ *BGT-planner* (Zhang et al., 2025), a state-of-the-art CMAB-based budget allocation framework; ⑤ *Threshold-based* (Li et al., 2023; Zhang et al., 2026), an online policy that selects actions based on a predicted utility-to-cost ratio, where multiple predicted cost dimensions are aggregated by averaging to adapt the original single-cost formulation ⑥ *Optimal*, an oracle-aided upper bound that makes decisions using perfect per-round reward and cost observations, representing the best achievable performance of M^2 -CMAB under ideal estimation. For ④ and ⑤, we adhere to the experimental settings and hyperparameter configurations reported in the original works.

5.2. Evaluation Configuration

Backbone Model. The scheduling policy is driven by a locally deployed *Qwen3-VL-2B-Instruct* model with a frozen backbone, which produces task-level multimodal representations for scheduling. Only lightweight reward and cost adapters are trained to predict the expected reward, latency, and monetary cost given the task context and candidate actions. When a local execution decision is selected, the cached intermediate states are reused and the original output head is invoked to directly generate the final response.

Budget regimes. We consider three budget regimes for both latency and monetary cost, derived from the aggregated cost of the five candidate actions. Specifically, *Restricted* sets the budget to the minimum aggregated cost value across all actions, *Normal* to the second-smallest aggregated cost, and *Generous* to the median aggregated cost.

Hyperparameters. The key hyperparameters used in the

scheduling and learning framework are summarized in Appendix E.3. In addition, we study the effect of the scheduling parameter T_0 through a sensitivity analysis on the fraction of rounds assigned to the initial phase.

5.3. Experimental Results and Analysis

Overall Performance Comparison (Answer for Q1).

Since each algorithm terminates upon exceeding either the latency or monetary budget, resulting in varying numbers of executed rounds, we adopt the **average inference reward** across executed rounds as the primary evaluation metric to ensure fair comparison. Each experiment is repeated five times with different random seeds to account for variability and ensure statistical reliability. As shown in Fig. 3, M^2 -CMAB consistently outperforms all realistic baselines across datasets and achieves performance closest to the oracle-aided upper bound. Notably, our method outperforms the second-best baseline by 6.79%, 13.08%, and 14.18% under the Restricted, Normal, and Generous budget regimes, respectively, on the COMPOSITE trace. These results underscore the effectiveness of the proposed representation and scheduling design in M^2 -CMAB for highly heterogeneous and complex MLLM inference workloads.

Moreover, as the budget increases, M^2 -CMAB achieves greater average improvements over the baselines, indicating that the algorithm can more effectively leverage additional scheduling flexibility to optimize performance. In some settings, the performance gap between M^2 -CMAB and the second-best baseline becomes smaller, particularly under highly constrained budgets (e.g., CoQA and GSM8K under

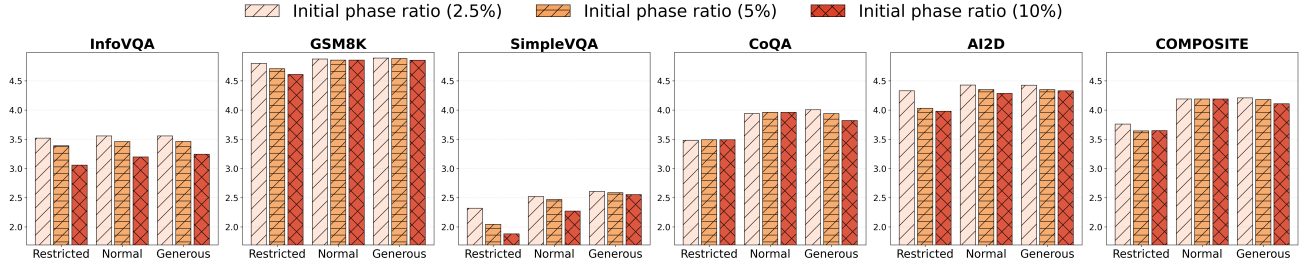


Figure 4. Sensitivity of M^2 -CMAB to the initial phase ratio, i.e., $\frac{(A+1)T_0}{T}$, evaluated by average inference reward (y-axis). Bars indicate the percentage of total rounds allocated to the initial phase, with three groups per subfigure corresponding to three budget regimes.

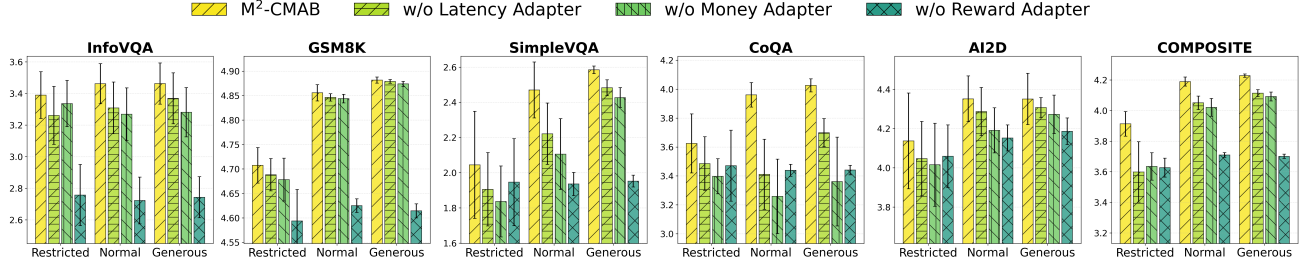


Figure 5. Ablation study of M^2 -CMAB across six datasets and three budget levels, illustrating the contribution of latency, money and reward predictor to the average inference reward (y-axis).

the Restricted setting) or when task rewards are relatively uniform across actions (e.g., GSM8K). The distributions of the datasets can be found in Appendix E.3. In these cases, the inherently limited room for task inference scheduling naturally reduces the potential performance margin across different decision policies. Notably, even under such challenging regimes, M^2 -CMAB remains very close to the Optimal oracle, with a gap below 1.2%, thereby demonstrating the robustness of the proposed approach in extreme and resource-constrained deployment scenarios.

Hyperparameter Sensitivity (Answer for Q2). We also conduct experiments to examine the effect of varying the initial phase ratio in Fig. 4. Specifically, we consider initial phase ratios of 2.5%, 5%, and 10% of the total rounds. Overall, M^2 -CMAB maintains stable and robust performance across a reasonable range of this hyperparameter, with a slight decrease in average inference reward as the initial phase ratio increases, particularly under the Restricted budget condition. This behavior can be attributed to the role of the initial phase: while allocating more rounds to this phase improves the accuracy of estimating the effective range of the constraint-control variables λ , it simultaneously reduces the number of rounds available for subsequent exploration and exploitation. This trade-off suggests that the length of the initial phase should be chosen in accordance with the underlying cost distribution and budget regime, rather than being set excessively large.

Ablation Study (Answer for Q3). To evaluate the contribution of each component in M^2 -CMAB, we perform ablation experiments on six datasets under three budget regimes. Specifically, we replace each key adapter-based predictor

with a random predictor while keeping the other components unchanged. As shown in Fig. 5, removing any component results in a performance drop relative to the complete version of our framework. In particular, removing the reward adapter from M^2 -CMAB leads to a more substantial performance degradation compared to the other adapters. This is likely because the Money and Latency adapters primarily function as predictors for budget constraints, and inaccuracies in one can be partially compensated by the other. However, accurate predictions from the Reward adapter are essential for effective scheduling decisions in M^2 -CMAB.

6. Conclusion

In this work, we address two fundamental challenges in MLLM inference scheduling: efficient task representation under heterogeneous modalities and effective resource utilization in online, budget-constrained settings. To this end, we propose M^2 -CMAB, an online scheduling framework for resource-constrained MLLM inference task. At its core, M^2 -CMAB employs a CLS-attentive multi-adapter *Predictor* for lightweight reward and cost estimation. A budget-aware *Constrainer* adjusts the relative importance of resource consumptions across rounds, enabling adaptive constraint handling. Building on these components, a two-phase *Scheduler* balances exploration and exploitation to ensure stable performance under diverse resource budgets. Future work will focus on establishing online regret guarantees for MLLM-based estimators used in the *Predictor*, and on exploring more lightweight and finer-grained representations of tasks and execution backends to further improve robustness and efficiency in large-scale MLLM deployments.

Impact Statement

This paper presents work whose goal is to advance the field of Machine Learning. There are many potential societal consequences of our work, none which we feel must be specifically highlighted here.

References

- Agrawal, S. and Devanur, N. R. Linear contextual bandits with knapsacks. In *Proceedings of the 30th International Conference on Neural Information Processing Systems (NIPS'16)*, pp. 3458–3467. Curran Associates Inc., 2016.
- Bai, S., Cai, Y., Chen, R., Chen, K., Chen, X., et al. Qwen3-vl technical report, 2025a. URL <https://arxiv.org/abs/2511.21631>.
- Bai, S., Chen, K., Liu, X., Wang, J., Ge, W., et al. Qwen2.5-vl technical report, 2025b. URL <https://arxiv.org/abs/2502.13923>.
- Chen, M., Zhang, B., Han, Z., Jiang, W., Wang, Y., Feng, S., Du, Y., and Bao, B. Test-Time Selective Adaptation for Uni-Modal Distribution Shift in Multi-Modal Data. In *Forty-second International Conference on Machine Learning (ICML 2025)*. PMLR, 2025.
- Cheng, X., Zhang, W., Zhang, S., Yang, J., Guan, X., Wu, X., Li, X., Zhang, G., Liu, J., Mai, Y., Zeng, Y., Wen, Z., Jin, K., Wang, B., Zhou, W., Lu, Y., Li, T., Huang, W., and Li, Z. Simplevqa: Multimodal factuality evaluation for multimodal large language models, 2025. URL <https://arxiv.org/abs/2502.13059>.
- Cobbe, K., Kosaraju, V., Bavarian, M., Chen, M., Jun, H., Kaiser, L., Plappert, M., Tworek, J., Hilton, J., Nakano, R., Hesse, C., and Schulman, J. Training verifiers to solve math word problems, 2021. URL <https://arxiv.org/abs/2110.14168>.
- Fei, H., Zhou, Y., Li, J., Li, X., Xu, Q., Li, B., Wu, S., Wang, Y., Zhou, J., Meng, J., Shi, Q., Zhou, Z., Shi, L., Gao, M., Zhang, D., Ge, Z., Tang, S., Pan, K., Ye, Y., Yuan, H., Zhang, T., Wu, W., Ju, T., Meng, Z., Xu, S., Jia, L., Hu, W., Luo, M., Luo, J., Chua, T., Yan, S., and Zhang, H. On Path to Multimodal Generalist: General-Level and General-Bench. In *Forty-second International Conference on Machine Learning (ICML 2025)*. PMLR, 2025.
- Fu, Y., Zhu, S., Su, R., Qiao, A., Stoica, I., and Zhang, H. Efficient LLM scheduling by learning to rank. In *Proceedings of the 38th International Conference on Neural Information Processing Systems (NIPS '24)*. Curran Associates Inc., 2024.
- Ge, C., Wang, X., Zhang, Z., Chen, H., Fan, J., Huang, L., Xue, H., and Zhu, W. Dynamic mixture of curriculum lora experts for continual multimodal instruction tuning. In *Forty-second International Conference on Machine Learning (ICML 2025)*. PMLR, 2025.
- Han, Y., Zeng, J., Wang, Y., Xiang, Y., and Zhang, J. Optimal Contextual Bandits with Knapsacks under Realizability via Regression Oracles. In *International Conference on AISTATS*, pp. 5011–5035. PMLR, 2023.
- Hazan, E. *Introduction to Online Convex Optimization*. Now Foundations and Trends, 2016. doi: 10.1561/24000000013.
- Huang, W., Liang, J., Shi, Z., Zhu, D., Wan, G., Li, H., Du, B., Tao, D., and Ye, M. Learn from Downstream and Be Yourself in Multimodal Large Language Models Fine-Tuning. In *Forty-second International Conference on Machine Learning (ICML 2025)*. PMLR, 2025.
- Jia, S., Frazier, P. I., and Kallus, N. Multi-Armed Bandits with Interference: Bridging Causal Inference and Adversarial Bandits. In *Forty-second International Conference on Machine Learning (ICML 2025)*. PMLR, 2025.
- Kembhavi, A., Salvato, M., Kolve, E., Seo, M., Hajishirzi, H., and Farhadi, A. A diagram is worth a dozen images, 2016. URL <https://arxiv.org/abs/1603.07396>.
- Li, B., Zhang, Y., Guo, D., Zhang, R., Li, F., Zhang, H., Zhang, K., Zhang, P., Li, Y., Liu, Z., and Li, C. Llava-onevision: Easy visual task transfer, 2024a. URL <https://arxiv.org/abs/2408.03326>.
- Li, F., Zhang, R., Zhang, H., Zhang, Y., Li, B., Li, W., Ma, Z., and Li, C. Llava-next-interleave: Tackling multi-image, video, and 3d in large multimodal models, 2024b. URL <https://arxiv.org/abs/2407.07895>.
- Li, S., Wang, H., Xu, W., Zhang, R., Guo, S., Yuan, J., Zhong, X., Zhang, T., and Li, R. Collaborative inference and learning between edge slms and cloud llms: A survey of algorithms, execution, and open challenges, 2025a. URL <https://arxiv.org/abs/2507.16731>.
- Li, S., Wang, H., Xu, W., Zhang, R., Guo, S., Yuan, J., Zhong, X., Zhang, T., and Li, R. Collaborative Inference and Learning between Edge SLMs and Cloud LLMs: A Survey of Algorithms, Execution, and Open Challenges, 2025b. URL <https://arxiv.org/abs/2507.16731>.
- Li, W., Xiang, L., Guo, B., Li, Z., and Wang, X. DPlanner: A Privacy Budgeting System for Utility. *IEEE Transactions on Information Forensics and Security*, 18:1196–1210, 2023.

- Li, Y. LLM Bandit: Cost-Efficient LLM Generation via Preference-Conditioned Dynamic Routing, 2025. URL <https://arxiv.org/abs/2502.02743>.
- Li, Y., Zhang, X., Hu, M., Wu, D., and Zhou, Y. W2CB: Online Data Acquisition Optimization With Wasserstein Contextual Combinatorial Bandits. *IEEE Transactions on Services Computing*, 18(6):4349–4363, 2025c.
- Lin, C.-Y. Rouge: A package for automatic evaluation of summaries. In *Text summarization branches out*, pp. 74–81, 2004.
- Liu, X., Dai, X., Zuo, J., Wang, S., Joe-Wong, C., Lui, J. C. S., and Chen, W. Offline Learning for Combinatorial Multi-armed Bandits. In *Forty-second International Conference on Machine Learning (ICML 2025)*. PMLR, 2025.
- Ma, Z., Zhang, S., Wei, L., and Tian, Q. Efficient Multimodal Long Context Learning for Training-free Adaptation. In *Forty-second International Conference on Machine Learning (ICML 2025)*. PMLR, 2025.
- Mathew, M., Bagal, V., Tito, R. P., Karatzas, D., Valveny, E., and Jawahar, C. V. Infographicvqa, 2021. URL <https://arxiv.org/abs/2104.12756>.
- Oh, C., Fang, Z., Im, S., Du, X., and Li, Y. Understanding Multimodal LLMs Under Distribution Shifts: An Information-Theoretic Approach. In *Forty-second International Conference on Machine Learning (ICML 2025)*. PMLR, 2025.
- Ouyang, T., Zhao, K., Zhang, X., Zhou, Z., and Chen, X. Dynamic Edge-centric Resource Provisioning for Online and Offline Services Co-location. In *IEEE Conference on Computer Communications (INFOCOM)*, pp. 1–10. IEEE, 2023.
- Pei, M., Shi, S., Zhang, L., Li, P., and Shen, S. GoIRL: Graph-Oriented Inverse Reinforcement Learning for Multimodal Trajectory Prediction. In *Forty-second International Conference on Machine Learning (ICML 2025)*. PMLR, 2025.
- Reddy, S., Chen, D., and Manning, C. D. CoQA: A Conversational Question Answering Challenge. *Transactions of the Association for Computational Linguistics*, 7:249–266, 2019.
- Shalev-Shwartz, S. Online Learning and Online Convex Optimization. *Foundations and Trends in Machine Learning*, 4(2):107–194, 2012.
- Tu, W., Deng, W., Campbell, D., Yao, Y., Zheng, J., Gedeon, T., and Liu, T. Ranked from within: Ranking large multimodal models without labels. In *Forty-second International Conference on Machine Learning (ICML 2025)*. PMLR, 2025.
- Wang, J., Zhao, S., Qiang, W., Li, J., Zheng, C., Sun, F., and Xiong, H. Towards the Causal Complete Cause of Multi-Modal Representation Learning. In *Forty-second International Conference on Machine Learning (ICML 2025)*. PMLR, 2025.
- Wu, H., Srikant, R., Liu, X., and Jiang, C. Algorithms with logarithmic or sublinear regret for constrained contextual bandits. In *Proceedings of International Conference on NeurIPS*, pp. 433–441. ACM, 2015.
- Wu, Q., Shao, Y., Wang, J., and Sun, X. Learning Optimal Multimodal Information Bottleneck Representations. In *Forty-second International Conference on Machine Learning (ICML 2025)*. PMLR, 2025.
- Xia, Y., Kong, F., Yu, T., Guo, L., Rossi, R. A., Kim, S., and Li, S. Which LLM to Play? Convergence-Aware Online Model Selection with Time-Increasing Bandits. In *Proceedings of the ACM Web Conference 2024 (WWW '24)*, pp. 4059–4070. ACM, 2024.
- Xu, Z., Nguyen, K. D., Mukherjee, P., Bagchi, S., Chatterji, S., Liang, Y., and Li, Y. Learning to inference adaptively for multimodal large language models. In *Proceedings of the IEEE/CVF International Conference on Computer Vision (ICCV)*, pp. 3552–3563. IEEE/CVF, 2025.
- Yang, Z., Yang, Y., Zhao, C., Guo, Q., He, W., and Ji, W. PerLLM: Personalized Inference Scheduling with Edge-Cloud Collaboration for Diverse LLM Services, 2024. URL <https://arxiv.org/abs/2405.14636>.
- Yang, Z., Guo, Q., Hu, Y., Zhao, C., Zhang, C., Zhao, J., and Ji, W. Moe-off: Adaptive heterogeneous modality-aware offloading with edge-cloud collaboration for efficient multimodal llm inference, 2025. URL <https://arxiv.org/abs/2509.16995>.
- Yuan, L., Han, D., Wang, S., and Brinton, C. Local-Cloud Inference Offloading for LLMs in Multi-Modal, Multi-Task, Multi-Dialogue Settings. In *Proceedings of the Twenty-sixth International Symposium on Theory, Algorithmic Foundations, and Protocol Design for Mobile Networks and Mobile Computing (MobiHoc'25)*, pp. 201–210. ACM, 2025.
- Zhang, X., Zhou, Y., Hu, M., Wu, D., Liao, P., Guizani, M., and Sheng, Q. Z. BGTplanner: Maximizing Training Accuracy for Differentially Private Federated Recommenders via Strategic Privacy Budget Allocation. *IEEE*

Transactions on Services Computing, 18(6):3523–3537, 2025.

Zhang, X., Zhou, Y., Wu, D., Sheng, Q. Z., Hu, M., and Xiao, L. PPVF: An Efficient Privacy-Preserving Online Video Fetching Framework With Correlated Differential Privacy. *IEEE Transactions on Networking*, 34:973–988, 2026.

Zhou, C., Liu, S., Yuan, X., Shi, J., Zhang, Y., and Pu, L. Libra: Novel llm token streaming via region-based task scheduling and token bundling. In *2025 IEEE/ACM 33rd International Symposium on Quality of Service (IWQoS)*, pp. 1–10, 2025.

A. Table of Main Notations

Table 1 provides the definitions of the main notations and symbols used throughout the paper to facilitate understanding and reference.

Table 1. Main notations and definitions.

Notation	Definition
t / T	Index of the online scheduling round and the total number of rounds.
Ω	Set of supported input modalities (e.g., text, vision, audio).
$\mathbf{x}^t = \{\mathbf{x}_\omega^t\}_{\omega \in \Omega}$	Multi-modal context of the task arriving at round t , consisting of modality-specific token embeddings.
$a^t \in \mathcal{A}$	Action selected at round t , corresponding to an MLLM inference configuration.
A	Cardinality of the action space.
r_a^t	Observed reward of executing action a under context \mathbf{x}^t at round t .
$\varphi_a^t \in \mathbb{R}_+^C$	Observed resource consumption (cost) vector of action a at round t over C constraint dimensions.
$\Phi \in \mathbb{R}_+^C$	Long-term budget vector across all resource dimensions.
$\mathcal{R}(a, \mathbf{x})$	Unknown expected reward function induced by action a and context \mathbf{x} .
$\mathcal{C}(a, \mathbf{x})$	Unknown expected cost function mapping an action-context pair to a C -dimensional resource consumption vector.
$\hat{r}_a^t = \hat{\mathcal{R}}(a, \mathbf{x}^t; \Theta_r^t)$	Predicted reward of action a at round t given by the adapter-based predictor.
$\hat{\varphi}_a^t = \hat{\mathcal{C}}(a, \mathbf{x}^t; \Theta_\varphi^t)$	A collection of C unknown cost functions, where each $\mathcal{C}(a, \mathbf{x}; \Theta_\varphi^{t,(c)})$ maps an action-context pair to the expected consumption of the c -th resource dimension.
$f_\vartheta(\cdot)$	Frozen MLLM backbone with parameter ϑ used to extract task-level multi-modal representations.
z_x^t	Task-level hidden representation obtained from CLS-attentive pooling over the frozen MLLM backbone at round t .
z_a	Embedding representation of action a .
Θ_r^t	Parameter set of the reward predictor at round t , consisting of the frozen MLLM backbone parameters ϑ and the trainable reward adapter parameters θ_r^t .
Θ_φ^t	Parameter set of the cost predictors at round t , given by $\{\Theta_\varphi^{t,(c)}\}_{c=1}^C$, where $\Theta_\varphi^{t,(c)} = \{\vartheta, \theta_\varphi^{t,(c)}\}$ denotes the parameters of the c -th cost adapter.
$\lambda^t \in \mathbb{R}_+^C$	Vector of dual variables (Lagrange multipliers) associated with long-term constraints at round t .
\mathcal{V}	Feasible domain of the dual variables with l_1 -radius Λ .
Λ	Radius of the dual feasible set, determined in the initial phase to control budget violation.
T_0	Number of exploration rounds per action in the initial phase of M ² -CMAB.
$\mathcal{S}_t(a)$	Predicted per-round Lagrangian score of action a at round t , combining reward and penalized cost.
$\mathcal{P}_t(a)$	Sampling probability of selecting action a at round t in the exploration–exploitation phase
$\text{Reg}(T)$	Regret of M ² -CMAB over T rounds, defined as $T \cdot \text{OPT} - \mathbb{E} \left[\sum_{t=1}^T r_{a^t}^t \right]$.
$\text{Reg}^r(T), \text{Reg}^c(T)$	Cumulative estimation regrets of the reward predictor and cost predictors over T rounds.
$\Phi_{\min} = \ \Phi^{-1}\ _\infty$	Minimum normalized budget parameter used in regret analysis and feasibility conditions.

B. Details of Adapter-Based Predictors

Context-Aware Representation Extraction. Given an action $a \in \mathcal{A}$, we consider the multi-modal context input $\mathbf{x}^t = \{\mathbf{x}_\omega^t\}_{\omega \in \Omega}$ together with the action embedding z_a to predict the corresponding reward and cost. To capture the intrinsic

semantic complexity of the task, we leverage a pre-trained multi-modal large language model (MLLM) backbone $f_{\vartheta}(\cdot)$ with frozen parameters ϑ , and extract a task-level representation z_x^t from the multi-modal context.

Specifically, an explicit [CLS] token is prepended to the multi-modal token sequence x^t as a global semantic anchor. From the selected output layer of the frozen backbone, we extract the multi-head self-attention tensor $\mathbf{I}^t \in \mathbb{R}^{H \times L \times L}$ and the hidden-state matrix $\mathbf{H}^t \in \mathbb{R}^{L \times d_{\text{hid}}}$, where H denotes the number of attention heads, L the token sequence length, and d_{hid} the hidden-state dimensionality.

For each attention head $h \in \{1, \dots, H\}$, we extract the attention weights from the [CLS] token to all tokens as

$$\alpha_h^t = \mathbf{I}_h^t[\text{CLS}, :] \in \mathbb{R}^L. \quad (11)$$

Using these weights, we perform attention-based pooling over the hidden states to obtain a head-wise semantic summary. To avoid introducing additional trainable parameters, the pooled representations across all heads are aggregated by simple averaging, yielding a compact, parameter-free context embedding

$$z_x^t = \frac{1}{H} \sum_{h=1}^H \frac{1}{L} \sum_{l=1}^L \alpha_{h,l}^t h_l^t, \quad (12)$$

where h_l^t denotes the l -th hidden-state vector from \mathbf{H}^t . The resulting representation z_x^t is used as the contextual feature fed into the bandit algorithm.

Backbone Model. The task backbone $f_{\vartheta}(\cdot)$ is instantiated using *Qwen3-VL-2B-Instruct*¹, a lightweight yet powerful multi-modal large language model capable of jointly processing text and visual inputs. Its parameters remain frozen throughout training, serving as a shared semantic encoder across all tasks and constraints.

Action Embedding. The embedding z_a of action a is obtained using a dedicated language embedding model, ensuring semantic alignment between the action description and the contextual representation. In our implementation, we employ *Qwen3-Embedding-0.6B*² to encode each candidate action into a fixed-dimensional vector, which is then concatenated with z_x^t for downstream prediction.

Adapter-Based Reward and Cost Prediction. Conditioned on both the context embedding z_x^t and the action embedding z_a , prediction is performed via lightweight task-specific adapters. Concretely, we concatenate the two embeddings and feed them into a set of adapters $\mathcal{F}_{\theta}(z_a \| z_x^t)$, parameterized by θ_r for reward prediction and $\{\theta_{\varphi}^{(c)}\}_{c=1}^C$ for per-dimension cost prediction.

Each adapter is instantiated as a lightweight multi-layer perceptron (MLP), whose detailed architecture is provided in the experimental section. Importantly, all adapters are trained while keeping the backbone parameters ϑ frozen, ensuring stable representation learning and efficient online updates.

Formally, the reward predictor is defined as

$$\hat{r}_a^t = \hat{\mathcal{R}}(a, x^t; \Theta_r^t), \quad \Theta_r^t = \{\vartheta, \theta_r^t\}, \quad (13)$$

and for each budget-constrained resource dimension $c \in \{1, \dots, C\}$, the corresponding cost predictor is given by

$$\hat{\varphi}_a^{t,(c)} = \hat{\mathcal{C}}(a, x^t; \Theta_{\varphi}^{t,(c)}), \quad \Theta_{\varphi}^{t,(c)} = \{\vartheta, \theta_{\varphi}^{t,(c)}\}. \quad (14)$$

The resulting vector $\hat{\varphi}_a^t$ characterizes the estimated per-round resource consumption associated with action a .

Training Objective. Both reward and cost adapters are trained using a unified regularized least-squares objective. Let \mathcal{F}_{θ} denote either a reward or a cost predictor, and let y^{τ} be the corresponding supervision signal, *i.e.*, reward r^{τ} or cost $\varphi^{\tau,(c)}$. The adapter parameters are updated by solving

$$\min_{\theta} \mathcal{J}(\theta) = \frac{1}{2|\Upsilon^t|} \sum_{\tau < t} (\mathcal{F}_{\theta} - y^{\tau})^2 + \frac{\lambda}{2} \|\theta - \theta^0\|_2^2, \quad (15)$$

¹<https://huggingface.co/Qwen/Qwen3-VL-2B-Instruct>

²<https://huggingface.co/Qwen/Qwen3-Embedding-0.6B>

Algorithm 1 Initial Phase of M^2 -CMAB for Estimating Dual Radius Λ

Input: Total rounds T ; exploration length T_0 ; action set \mathcal{A} with $|\mathcal{A}| = A$.

Output: Estimated dual radius Λ ; historical dataset $\Upsilon^{(A+1)T_0}$.

- 1: Initialize historical dataset $\Upsilon^0 \leftarrow \emptyset$.
 - // Stage I //
 - 2: Initialize action counters $n_a \leftarrow T_0$, for all $a \in \mathcal{A}$.
 - 3: Initialize historical dataset $\Upsilon^0 \leftarrow \emptyset$.
 - 4: **for** $t = 1$ **to** $A \cdot T_0$ **do**
 - 5: Observe multi-modal context $\mathbf{x}^t = \{\mathbf{x}_\omega^t\}_{\omega \in \Omega}$.
 - 6: Randomly sample an action a^t from $\{a \in \mathcal{A} : n_a > 0\}$.
 - 7: Execute action a^t and observe reward r_a^t and cost vector $\boldsymbol{\varphi}^t$ for all budgets.
 - 8: Update counter $n_{a^t} \leftarrow n_{a^t} - 1$.
 - 9: Update dataset $\Upsilon^t \leftarrow \Upsilon^{t-1} \cup \{(r^t, \boldsymbol{\varphi}^t, a^t, \mathbf{x}^t)\}$.
 - 10: **end for**
 - // Stage II //
 - 11: **for** $t = AT_0 + 1$ **to** $(A + 1)T_0$ **do**
 - 12: Select an exploratory action $a^t \in \mathcal{A}$.
 - 13: Observe multi-modal context \mathbf{x}^t .
 - 14: Observe reward r_a^t and cost vector $\boldsymbol{\varphi}^t$ for all budgets.
 - 15: Update dataset $\Upsilon^t \leftarrow \Upsilon^{t-1} \cup \{(r^t, \boldsymbol{\varphi}^t, a^t, \mathbf{x}^t)\}$.
 - 16: Compute predicted rewards $\hat{r}_a^t = \hat{\mathcal{R}}(a, \mathbf{x}^t; \boldsymbol{\Theta}_r^t)$ for all $a \in \mathcal{A} / a^t$.
 - 17: **for** $c = 0$ **to** $C - 1$ **do**
 - 18: Compute predicted cost $\hat{\varphi}_a^{t,(c)} = \hat{\mathcal{C}}(a, \mathbf{x}^t; \boldsymbol{\Theta}_\varphi^{t,(c)})$ for all $a \in \mathcal{A} / a^t$.
 - 19: **end for**
 - 20: **end for**
 - 21: Estimate $\hat{\text{OPT}}(T_0)$ by solving the linear program defined in Eq. (6).
 - 22: Set the dual radius $\Lambda = \frac{T}{\Phi_{\min}} \left(\hat{\text{OPT}}(T_0) + \mathcal{M}(T_0) \right)$, where $\Phi_{\min} = \|\boldsymbol{\Phi}^{-1}\|_\infty$ and $\mathcal{M}(T_0)$ is defined in Eq. (6c).
-

where $\Upsilon^t = \{(r^\tau, \boldsymbol{\varphi}^\tau, a^\tau, \mathbf{x}^\tau) \mid \tau < t, \tau \in \mathbb{N}_+\}$ denotes the historical observation set, $\boldsymbol{\theta}^0$ is the initialization of adapter parameters, and $\lambda > 0$ controls the regularization strength.

C. Initial Phase of M^2 -CMAB

This appendix describes the initial phase of M^2 -CMAB, which is designed to determine the radius Λ of the dual feasible set $\mathcal{V} = \{\boldsymbol{\lambda} \in \mathbb{R}_+^C : \|\boldsymbol{\lambda}\|_1 \leq \Lambda\}$. The purpose of this phase is to ensure sufficient exploration of the action space and to obtain a reliable estimate of the optimal value required for subsequent dual-based exploration–exploitation.

The initial phase consists of two sequential stages. First, each action $a \in \mathcal{A}$ is executed for T_0 rounds to collect context–reward observations, which are used to fit a regression model for estimating the unknown expected reward function $\mathcal{R}(a, \mathbf{x})$ and reward functions $\mathcal{C}(a, \mathbf{x})$. Second, an additional exploration stage is conducted to refine the reward estimator and to compute an empirical estimate of the optimal value $\hat{\text{OPT}}(T_0)$, based on which the dual radius Λ is determined.

Throughout this phase, only observed rewards are used for estimation, and no dual variables are updated. The collected historical data serve as a warm-start for both the predictor initialization and the dual-constrained optimization in the main phase.

D. Regret Analysis Details

This appendix establishes the regret guarantees of M^2 -CMAB shown in Alg. 2 in Theorem 4.1. We begin by specifying the stochastic data-generating process and the class of admissible reward and cost functions. We then define the optimal static benchmark policy and its associated value, which serves as the comparator in the regret definition. Under these preliminaries, the regret analysis proceeds by bounding the error introduced by function estimation and dual-based decision making.

Algorithm 2 The M^2 -CMAB Algorithm

Require: Total rounds T ; Exploration rounds T_0 .

- 1: Determine the dual radius Λ via the initial phase (Alg. 1) and obtain the historical set $\Upsilon^{(A+1) \cdot T_0}$;
- 2: Initialize the dual variable $\lambda^1 \in \mathcal{V}$;
- 3: **for** $t = (A + 1) \cdot T_0 + 1, \dots, T$ **do**
- 4: Observe the context of the t -th task \mathbf{x}^t ;
- 5: **// Step ①: Generating Action Scores //**
- 6: Use the reward and cost predictors to estimate the expected reward \hat{r}_a^t and cost vector $\hat{\varphi}_a^t$ for all $a \in \mathcal{A}$ based on \mathbf{x}^t and action embeddings;
- 7: Compute the per-round Lagrangian score $\mathcal{S}^t(a)$ for each action $a \in \mathcal{A}$ using the current dual variable λ^t ;
- 8: **// Step ②: Selecting the Optimal Action //**
- 9: Construct the action sampling distribution $\mathcal{P}^t(\cdot)$ according to the scores $\{\mathcal{S}^t(a)\}_{a \in \mathcal{A}}$;
- 10: Sample the scheduling action $a^t \sim \mathcal{P}^t$;
- 11: **// Step ③: Updating Penalties //**
- 12: Observe the realized reward r^t and cost vector φ^t , and update the historical set $\Upsilon^t \leftarrow \Upsilon^{t-1} \cup (r^t, \varphi^t, a^t, \mathbf{x}^t)$;
- 13: Update the reward and cost adapter parameters using Υ^t according to the prescribed update rules;
- 14: Update the dual variable λ^{t+1} via OMD method;
- 15: **end for**

Proof. We first formalize the stochastic environment through a realizability assumption on the underlying reward and cost functions.

Assumption D.1 (Realizability of Reward and Cost Functions). There exist some optimal regression functions $\hat{\mathcal{R}}^*$ and $\hat{\mathcal{C}}^*$ characterizing the expected reward and cost distributions, respectively, such that for any round and any action $a \in \mathcal{A}$,

$$\mathbb{E}[r_a \mid \mathbf{x}] = \hat{\mathcal{R}}^*(a, \mathbf{x}), \quad \mathbb{E}[\varphi_a \mid \mathbf{x}] = \hat{\mathcal{C}}^*(a, \mathbf{x}),$$

where $\mathbf{x} = \{\mathbf{x}_\omega\}_{\omega \in \Omega}$ is the observed multi-modal context.

Under Assumption D.1, the stochastic reward and cost processes admit well-defined expected functions induced by the action–context pair. This allows us to characterize the performance of an online policy through comparison with an optimal static benchmark that has full knowledge of these expectations.

Definition D.2 (Optimal Static Benchmark Value). Based on the realizable expected reward and cost functions in Assumption D.1, let $\pi^* : \mathcal{X} \rightarrow P_{\mathcal{A}}$ be a static randomized policy that maps each context $\mathbf{x} \in \mathcal{X}$ to a probability distribution over the action set \mathcal{A} and $\mathbf{1}$ represent the all-ones vector. Then, OPT is defined as

$$\begin{aligned} \text{OPT} &\triangleq \max_{\pi^*} \mathbb{E}_{\mathbf{x} \sim \mathcal{X}} \left[\sum_{a \in \mathcal{A}} \pi^*(\mathbf{x}) \hat{\mathcal{R}}^*(a, \mathbf{x}) \right], \\ \text{s.t. } &\mathbb{E}_{\mathbf{x} \sim \mathcal{X}} \left[\sum_{a \in \mathcal{A}} \pi^*(\mathbf{x}) \frac{\hat{\mathcal{C}}^*(a, \mathbf{x})}{\Phi} \right] \leq \frac{\mathbf{1}}{T}. \end{aligned} \tag{16}$$

The benchmark value OPT characterizes the maximum achievable expected reward under the long-term budget constraints in hindsight. We now use this benchmark to formally define the regret of the M^2 -CMAB algorithm.

Definition D.3 (Cumulative Regret of the Online Algorithm). Given the optimal static benchmark value OPT defined in Definition D.2, the regret of M^2 -CMAB over T rounds is defined as

$$\text{Reg}(T) \triangleq T \cdot \text{OPT} - \mathbb{E} \left[\sum_{t=1}^T r_a^t \right], \tag{17}$$

where $T \cdot \text{OPT}$ upper bounds the optimal cumulative reward achievable in online scenarios (Agrawal & Devanur, 2016).

To analyze $\text{Reg}(T)$, it remains to quantify the error introduced by learning-based estimation of the reward and cost functions. We next formalize this error through squared-loss estimation regret.

Definition D.4 (Squared-Loss Estimation Regret). The squared-loss estimation regret of the reward predictor $\hat{\mathcal{R}}(\cdot, \cdot)$ over T rounds is defined as

$$\text{Reg}^r(T) \triangleq \sum_{t=1}^T \left(\hat{\mathcal{R}}(a^t, \mathbf{x}^t; \Theta_r^t) - \hat{\mathcal{R}}^*(a^t, \mathbf{x}^t) \right)^2. \quad (18)$$

Similarly, the squared-loss estimation regret of the cost predictors $\hat{\mathcal{C}}(\cdot, \cdot)$ is defined as

$$\text{Reg}^c(T) \triangleq \sum_{t=1}^T \left\| \hat{\mathcal{C}}(a^t, \mathbf{x}^t; \Theta_\varphi^t) - \hat{\mathcal{C}}^*(a^t, \mathbf{x}^t) \right\|_2^2. \quad (19)$$

With the regret benchmark and estimation error measures in place, we are ready to analyze the regret incurred during the exploration–exploitation (main) phase of M^2 -CMAB. The following lemma characterizes the regret contribution of this phase when the dual variables are updated within a bounded feasible set.

Lemma D.5 (Regret Bound of SquareCBwK, Theorem A.1 (Han et al., 2023)). *Consider the exploration-exploitation execution of M^2 -CMAB following SquareCBwK algorithm (Han et al., 2023), where the dual variables are updated over the feasible set*

$$\mathcal{V} = \{ \boldsymbol{\lambda} \in \mathbb{R}_+^C : \|\boldsymbol{\lambda}\|_1 \leq \Lambda \},$$

with a fixed radius Λ determined in the initial phase. Then the regret incurred during the exploration-exploitation admits the bound

$$\text{Reg}(T) \lesssim (\Lambda + 1) \sqrt{AT \left(\text{Reg}^r(T) + \text{Reg}^c(T) + \log(CT) \right)}. \quad (20)$$

Lemma D.5 characterizes the regret incurred during the exploration–exploitation phase when the dual variables are updated within a fixed feasible radius Λ . To make this result applicable, it remains to show that the dual radius Λ , estimated in the initial phase, is well controlled with high probability. To this end, we establish a concentration guarantee for the estimation of the ℓ_1 -radius Λ .

Lemma D.6 (Accuracy of the Estimated Dual Radius, Lemma 4.1 (Han et al., 2023)). *Denoting the optimal value of (6) by $OPT(T_0)$, and setting $\Lambda = \frac{T}{\Phi_{\min}} \left(OPT(T_0) + M(T_0) \right)$, where $\Phi_{\min} = \|\Phi_{\min}^{-1}\|_\infty$, we have with probability at least $1 - O(1/T^2)$,*

$$\frac{T \cdot OPT}{\Phi_{\min}} \leq \Lambda \leq \left(\frac{6T \cdot \mathcal{M}(T_0)}{\Phi_{\min}} + 1 \right) \left(\frac{T \cdot OPT}{\Phi_{\min}} + 1 \right), \quad (21)$$

Lemma D.6 establishes a high-probability bound on the ℓ_1 -radius Λ estimated in the initial phase. In particular, when the normalized budget parameter satisfies $\Phi_{\min} = O(T \cdot \mathcal{M}(T_0))$, the upper bound in Lemma D.6 implies that the dual radius can be simplified as

$$\Lambda \lesssim \frac{T \cdot OPT}{\Phi_{\min}} + 1, \quad (22)$$

where the notation “ \lesssim ” denotes an inequality up to a universal constant factor. With this estimation accuracy of Λ , the online mirror descent (OMD) algorithm used to update the dual variable $\boldsymbol{\lambda}$ achieves an $O(\sqrt{T})$ regret guarantee, as shown in Lemma 2.2 of (Han et al., 2023).

Substituting the above estimate of Λ into the regret bound of the exploration–exploitation phase given in Lemma D.5, we obtain the following high-probability regret guarantee for the exploration–exploitation phase of M^2 -CMAB:

$$\text{Reg}^{\text{ee}}(T) \lesssim \left(\frac{T \cdot OPT}{\Phi_{\min}} + 1 \right) \sqrt{AT \left(\text{Reg}^r(T) + \text{Reg}^c(T) + \log(CT) \right)}. \quad (23)$$

Table 2. Key hyperparameters used in the scheduling framework (placeholders).

Hyperparameters	Description
P_{local}	Average power consumption of the local device (W), 600
κ	Electricity price coefficient (cost per Joule), 2.06e-8

Regret decomposition across phases. In the initial phase (Alg. 1), the algorithm runs for AT_0 rounds to estimate a feasible dual radius. During this phase, the expected per-round regret is upper bounded by the optimal dual radius Λ . By Lemma D.6, with high probability $\Lambda \lesssim \frac{T \cdot \text{OPT}}{\Phi_{\min}} + 1$, which implies that the total regret incurred in the initial phase is at most

$$\text{Reg}^{\text{ini}}(T) \lesssim \left(\frac{T \cdot \text{OPT}}{\Phi_{\min}} + 1 \right) AT_0. \quad (24)$$

Combining the regret contributions from the initial phase and the exploration–exploitation phase, we conclude that the total regret of M^2 -CMAB satisfies

$$\text{Reg}(T) = \text{Reg}^{\text{ini}}(T) + \text{Reg}^{\text{ee}}(T) \lesssim \left(\frac{T \cdot \text{OPT}}{\Phi_{\min}} + 1 \right) \left(AT_0 + \sqrt{AT[\text{Reg}^r(T) + \text{Reg}^c(T) + \log(CT)]} \right). \quad (25)$$

Therefore, we obtain the regret guarantee stated in Theorem 4.1 for M^2 -CMAB in Algorithm 2. \square

E. Supplement for Experiments

E.1. Distribution of Reward, Latency, and Monetary Cost Across Individual Datasets.

Figure 6 illustrates the distribution of reward, latency, and monetary cost across MLLM inference backends for the five individual datasets as well as the composite dataset.

E.2. Simulation Metrics and Reward Definitions

This appendix presents the formal mathematical definitions of the latency, monetary cost, and response quality (reward) metrics used throughout the experimental evaluation.

Local Execution. For local execution, inference latency is modeled as

$$\psi_{\text{Local}} = \frac{T_{\text{in}} + T_{\text{out}}}{\text{FLOPS}_{\text{device}}}, \quad (26)$$

where T_{in} and T_{out} denote the numbers of input and output tokens, respectively, and $\text{FLOPS}_{\text{device}}$ is the effective compute throughput of the local device. The corresponding monetary cost is defined as

$$\phi_{\text{Local}} = \psi_{\text{Local}} \cdot P_{\text{local}} \cdot \kappa, \quad (27)$$

where P_{local} denotes the average power consumption of the device and κ is the electricity price coefficient.

Cloud Execution. For cloud execution, inference latency ψ_{Cloud} is modeled as the sum of network transmission delay and backend inference time, calibrated using empirical API traces. The monetary cost of cloud execution is computed as

$$\phi_{\text{Cloud}} = C_{\text{in}} + C_{\text{out}} + C_{\text{img}}, \quad (28)$$

where C_{in} and C_{out} denote provider-specific input and output token charges, and C_{img} captures modality-dependent processing costs (e.g., image inputs).

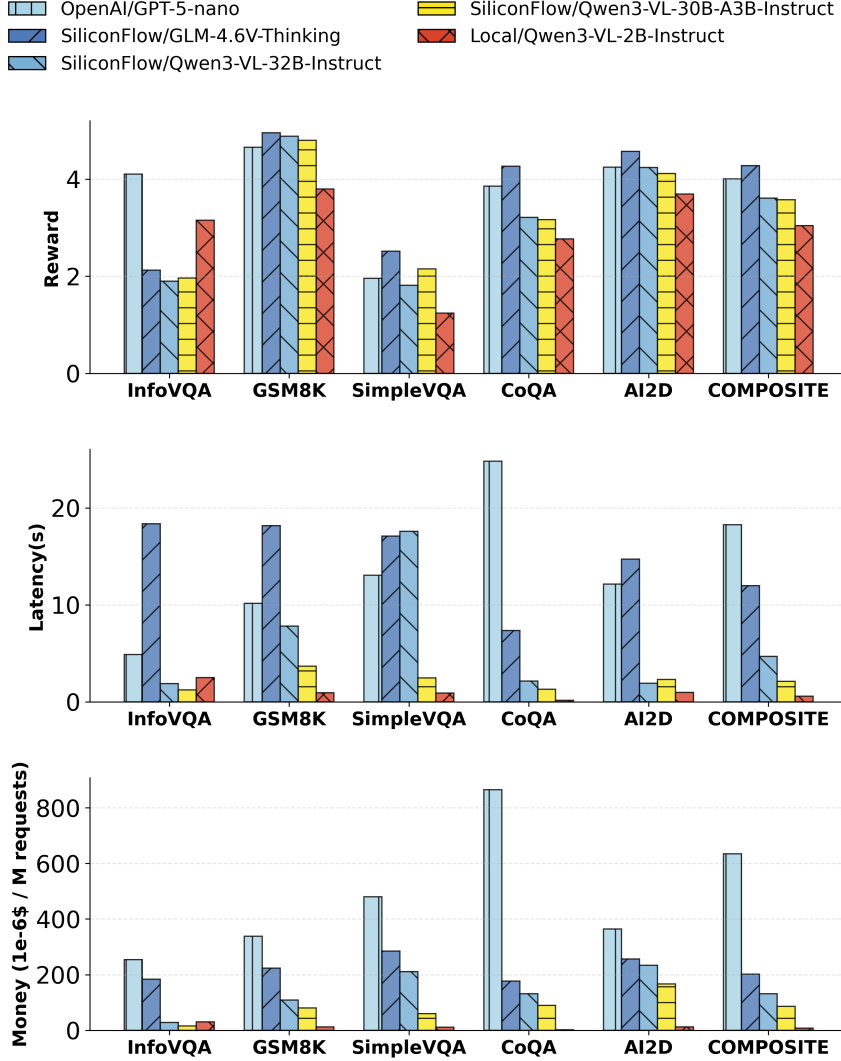


Figure 6. Comparison of reward, latency, and monetary cost across MLLM inference backends on individual datasets and a mixed multi-modal task trace.

Response Quality and Reward Definition. We define the response quality, denoted by $r \in [1, 5]$, as the reward signal used to evaluate inference outcomes across different datasets. Due to the heterogeneity of task formats and supervision levels, the reward is computed in a dataset-specific manner and normalized to ensure cross-dataset comparability. For standard generative QA tasks (e.g. CoQA), we compute the reward based on the similarity between the model-generated text and the reference answer. Specifically, we use the ROUGE-L (Lin, 2004) score and map it to an integer reward in $[1, 5]$ according to Table 3.

For multiple-choice tasks, where all candidate options (including the correct answer) are provided in the prompt (e.g. AI2D), we adopt exact-match evaluation. If the model’s selected answer matches the ground-truth option, a reward of 5 is assigned; otherwise, the reward is set to 1. This design ensures that the reward function is normalized and comparable across different task formats, facilitating consistent learning and scheduling within the M^2 -CMAB framework.

E.3. Additional Implementation Details

We provide further details on baseline implementations, dataset preprocessing, and hardware specifications in this appendix to ensure full reproducibility. All experiments are conducted under identical workload traces and budget constraints.

Table 2 summarizes the key hyperparameters involved in the scheduling and learning framework. We report them here for completeness and reproducibility. Unless otherwise specified, these hyperparameters are shared across all experiments.

Table 3. Mapping from ROUGE-L scores to discrete reward levels.

ROUGE-L	Reward
0	1
(0, 0.15)	2
[0.15, 3)	3
[0.3, 0.4)	4
(0.4, 1]	5

Table 4. Execution models used in the scheduling action space.

Category	Model	Provider / Deployment
Local	Qwen3-VL-2B-Instruct	On-device
Cloud	GPT-5-nano	OpenAI API
Cloud	Qwen3-VL-32B-Instruct	SiliconFlow API
Cloud	Qwen3-VL-30B-A3B-Instruct	On-device
Cloud	GLM-4.6V-Thinking	SiliconFlow API

E.4. Execution Backend Configurations

Table 4 summarizes all execution backends considered in our action space, including their deployment location and provider.

E.5. Prompt Used in Experiments

AI2D

You are an assistant that answers questions based on a given image. Generate the answer in the format "Option x" (x is the correct option index/letter).
 Image: {image}
 Question: {question}
 Options: {options}

CoQA

You are an assistant that answers questions based on a given story. Use only the information from the story to provide concise answers without adding extra content.
 Backstory: {story}
 Question: {question}

GSM8K

You are a math expert. Please answer the given math problem.
 Generate the results strictly in the following format:
 "Analysis: Your Analysis Process. Answer: Your final answer to the question."
 Question: {question}

InfoVQA & SimpleVQA

You are an assistant that answers questions based on a given image. Provide concise answers without adding any extra content.
 Image: {image}\n
 Question: {question}